

Structural Studies on $\text{Ba}_2\text{SrMg}_4\text{F}_{14}$ and $\text{Ba}_2\text{MM}'\text{Mg}_4\text{F}_{14}$ ($M = \text{Ca}, \text{Sr}, \text{Ba}$)

Frank Kubel, Nicole Wandl, and Mariana Pantazi

Institute of Chemical Technologies and Analytics, Vienna University of Technology,
Getreidemarkt 9/164-SC, A-1060 Vienna, Austria

Reprint requests to Prof. F. Kubel. Fax: +43 (1) 58801-171 99. E-mail: frank.kubel@tuwien.ac.at

Z. Naturforsch. **2012**, *67b*, 70–74; received November 18, 2011

The new barium strontium magnesium fluoride $\text{Ba}_2\text{SrMg}_4\text{F}_{14}$ has been prepared as an almost single-phase colorless powder by precipitating amorphous precursors and heating them at 650 °C. The compound crystallizes in the space group $P4_2/mnm$ (no. 136) with $a = 12.45514(4)$, $c = 7.46092(3)$ Å, $V = 1157.42(1)$ Å³ and $Z = 4$. It is isostructural with the previously known Ca analog, $\text{Ba}_{2.2}\text{Ca}_{0.8}\text{Mg}_4\text{F}_{14}$. The structure is built up from a channel-forming network of tetrahedral $(\text{MgF}_6)_4$ units linked by bridging fluorine atoms. The channels contain the Ba^{2+} ions (CN = 11) and Sr^{2+} ions (CN = 8, CaF_2 type-related environment). Solid solutions with composition $\text{Ba}_2(\text{Sr}_{1-x}\text{Ca}_x)\text{Mg}_4\text{F}_{14}$ with $x = 0.13(1)$, $0.36(1)$ and $0.51(1)$ as well as $\text{Ba}_2(\text{Sr}_{0.83(1)}\text{Ba}_{0.17(1)})\text{Mg}_4\text{F}_{14}$ were synthesized and characterized by powder X-ray diffraction.

Key words: Barium Strontium Calcium Magnesium Fluorides, Precursor Chemistry, Solid Solutions, Cluster-like Units

Introduction

During our research on new luminescent materials, an unknown barium calcium magnesium fluoride and a compound stabilized as a solid solution $\text{Ba}_2(\text{Ba}_{0.2}\text{Ca}_{0.8})\text{Mg}_4\text{F}_{14}$ were characterized by single-crystal X-ray diffraction. Supported by structural and geometrical arguments, other compositions can be predicted where $\text{Ba}^{2+}/\text{Ca}^{2+}$ is partially or fully replaced with Sr^{2+} to give $\text{Ba}_2\text{SrMg}_4\text{F}_{14}$ as an ordered variant. This family of compounds is of interest regarding the photophysical properties, as rare earth ions can be introduced into the channels to form new phosphors [1]. The understanding of solid solutions is important to determine the color response on activating the rare earth ion by UV light in different crystal fields. It is furthermore relevant from a theoretical point for studies of the stability range of these structures.

Experimental Section

Synthesis of $\text{Ba}_2\text{SrMg}_4\text{F}_{14}$

The compound $\text{Ba}_2\text{SrMg}_4\text{F}_{14}$ was synthesized in a two-step reaction from freshly precipitated XRD-amorphous fluoride precursors according to [1]. From an aqueous solution of $\text{Ba}(\text{OH})_2 \cdot 8\text{H}_2\text{O}$, $\text{Sr}(\text{OH})_2 \cdot 8\text{H}_2\text{O}$ and $\text{Mg}(\text{CH}_3\text{COO})_2 \cdot 4\text{H}_2\text{O}$ the fluorides were precipitated with NH_4F , washed with water and ethanol, then dried at r. t. for

two days and heated at 100 °C for 4.5 h. The compound was obtained as a colorless powder after heating at 650 °C for 3 h in a covered platinum crucible in the presence of small amounts of NH_4F to prevent the formation of oxides. The synthesis by ceramic methods from pellets of carefully milled and mixed BaF_2 , MgF_2 and SrF_2 powders following the same procedure failed to give a single-phase product. After heating a sample two times for 96 h at 650 °C and 700 °C, respectively, the diffraction pattern showed only 14 % of the title compound.

Quantitative EDX measurements of the product gave a Ba to Sr to Mg ratio of 2 to 0.95 to 3.9 close to the theoretical values. The underestimated value of 8.8 (expected 14) for fluorine is due to the limits of the method.

Synthesis of $\text{Ba}_2\text{MM}'\text{Mg}_4\text{F}_{14}$ ($M = \text{Ba}, \text{Sr}, \text{Ca}$)

For the syntheses of the solid solutions $\text{Ba}_2(\text{Sr}_{x-1}\text{Ca}_x)\text{Mg}_4\text{F}_{14}$ (up to $x \sim 0.5$), $\text{Ca}(\text{CH}_3\text{COO})_2$ was used. $\text{Ba}_2(\text{Sr}_{0.8}\text{Ba}_{0.2})\text{Mg}_4\text{F}_{14}$ was synthesized from stoichiometric precursors.

X-Ray structure analysis (powder diffraction)

Powder diffraction patterns were collected on a Philips X'Pert Bragg Brentano diffractometer with $\text{CuK}\alpha$ radiation, primary and secondary Soller slits of 0.04 rad, a divergence slit of 0.5°, a fixed antiscatter slit of 1° and a 200 mm goniometer radius. A standard steel holder for flat samples was used. Intensities were measured at r. t. using an

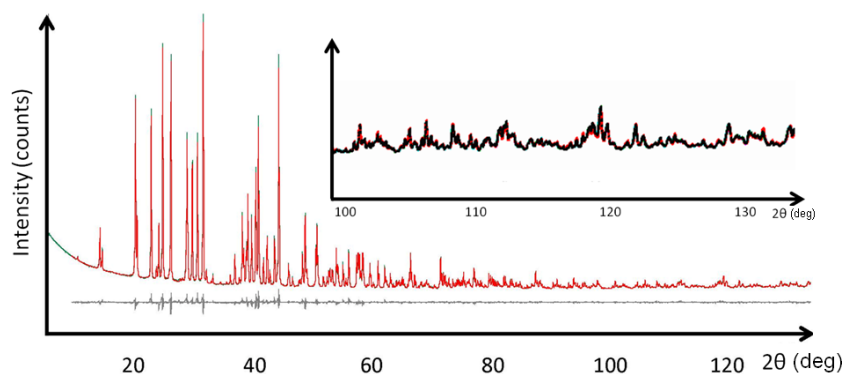


Fig. 1 (color online). Rietveld refinement (observed, calculated and difference pattern) of a Ba₂SrMg₄F₁₄ sample. Intensities in the range between 100 and 135° in 2θ (CuK α radiation). A portion of the diffraction pattern shows intensities magnified by a factor of 9.

X'Celerator detector with a NiK β filter and a scan length of *ca.* 2.55°. The evaluation and Rietveld refinements with the fundamental parameters approach were performed with the TOPAS 4.2 software [2].

Further details of the crystal structure investigation may be obtained from Fachinformationszentrum Karlsruhe, 76344 Eggenstein-Leopoldshafen, Germany (fax: +49-7247-808-666; e-mail: crysdata@fiz-karlsruhe.de, http://www.fiz-informationsdienste.de/en/DB/icsd/depot_anforderung.html) on quoting the deposition number CSD-423762.

Thermal analysis

Caloric measurements were carried out using a Netzsch STA 449 C Jupiter system in DTA/TG mode with Al₂O₃ crucibles in Ar atmosphere, thermogravimetric measurements on a Netzsch TG 209 F3 Tarsus instrument in a nitrogen atmosphere. The IR spectra were measured on a Perkin Elmer Spectrum 65 instrument with 4 scans and a resolution of 4 cm⁻¹, in a range of 4000–500 cm⁻¹. SEM and EDX measurements were carried out using an FEI Quanta 200 instrument.

Results and Discussion

Freshly precipitated fluorine precursors were found to be amorphous from XRD patterns and SEM photos. The high surface and reactivity can be used to synthesize Ba₂SrMg₄F₁₄ at 650 °C in 3 h. Low-temperature thermogravimetric measurements showed a weight loss of adsorbed water up to 500 °C in three steps. Between 500 and 700 °C no weight loss was observed; above 700 °C, small losses occurred. The latter might be related to OH groups incorporated in the structure during synthesis under impure N₂ as protecting atmosphere and not NH₄F as used during the synthesis in a Pt crucible. To verify the presence of OH groups within the title compound, IR measurements were carried out. No indication of water or

OH groups was observed, however. XRD measurements revealed an almost single-phase product. As can be seen from the Rietveld refinement of the diffraction pattern, Fig. 1, the main impurity is (Ba,Sr)MgF₄ with less than 0.5 wt.-%. The refinement after conventional solid-state synthesis gave max. 14 % of the title compound together with 70 % (Ba_{0.7}Sr_{0.3})MgF₄, 6 % MgF₂ and 10 % SrF₂. SEM photos showed the transformation from amorphous precursors to crystalline materials with a crystallite size of ~ 500 nm. The EDX element analysis confirmed the stoichiometry of Ba₂SrMg₄F₁₄.

To determine the temperature stability range of the compound, a DSC analysis was carried out up to 850 °C, but gave no clear signals indicating decomposition. Heating experiments followed by XRD analysis showed the stability of Ba₂SrMg₄F₁₄ between 500 and 700 °C. At higher temperatures it decomposes to (Ba,Sr)MgF₄. After melting at ~ 850 °C, Ba_{0.5}Sr_{0.5}MgF₄ (26 %), Ba₆Mg₇F₁₂ (44 %) and MgF₂ (30 % by weight) were observed. Attempts to grow single crystals by prolonged heating at 650 or 700 °C were unsuccessful.

Structural data were obtained by Rietveld refinements starting with the parameters of Ba₂Ba_{0.2}Ca_{0.8}Mg₄F₁₄ [1]. Crystal data are summarized in Table 1. Table 2 shows the refined atomic positions; Table 3 gives selected interatomic distances.

The structure can be described as a regular MgF₆ network with isolated Mg₄ cluster-like units. To compare different MgF₆ networks from literature data, distances Mg–Mg are considered in a first approach. Two types of connections can be observed: Mg–Mg distances for edge-sharing octahedra are between 2.9–3.1 Å as observed for Ba₂Mg₃F₁₀ [3], Ba₆Mg₇F₂₆ [4] and Ba₆Mg₁₁F₃₄ [5] or MgF₂ [6]. The distances

Table 1. Crystal structure data for Ba₂SrMg₄F₁₄.

| | |
|---|---|
| Formula | Ba ₂ SrMg ₄ F ₁₄ |
| M_r | 725.52 |
| Crystal size: diameter, nm | 334(4) |
| Crystal system | tetragonal |
| Space group | $P4_2/mmm$ (no.136) |
| $a, b, \text{\AA}$ | 12.45514(4) |
| $c, \text{\AA}$ | 7.46092(3) |
| $V, \text{\AA}^3$ | 1157.42(1) |
| Z | 4 |
| $D_{\text{calc}}, \text{g cm}^{-3}$ | 4.16 |
| $\mu(\text{CuK}\alpha), \text{cm}^{-1}$ | 621.8 |
| $F(000), e$ | 1296 |
| 2θ range, deg | 5 – 135 |
| Parameters refined | 36 |
| $R_p / wR_p(I) / R_{\text{Bragg}}, \%$ | 3.5 / 4.9 / 1.6 |
| GoF (F^2) | 3.54 |
| CSD no. | 423762 |

Table 2. Atomic positional parameters for Ba₂SrMg₄F₁₄^a.

| Atom | Wyckoff | x | y | z | $B_{\text{iso}}(\text{\AA}^2)$ |
|------|---------|------------|------------|-----------|--------------------------------|
| Ba | 8j | 0.02000(4) | 0.31107(5) | 0 | 1.46(2) |
| Sr | 4e | 0 | 0 | 0.2466(1) | 0.73(3) |
| Mg1 | 8j | 0.2962(2) | 0.2962(2) | 0.2461(4) | 0.95(4)+ |
| Mg2 | 8i | 0.2461(2) | 0.5485(2) | 0 | 0.95(4)+ |
| F1 | 16k | 0.1449(2) | 0.3087(3) | 0.3096(4) | 1.36(4)* |
| F2 | 16k | 0.3001(2) | 0.4549(2) | 0.1970(4) | 1.36(4)* |
| F3 | 8i | 0.1081(3) | 0.4896(4) | 0 | 1.36(4)* |
| F4 | 4g | 0.1630(3) | \bar{x} | 0 | 1.36(4)* |
| F5 | 4g | 0.4013(3) | \bar{x} | 0 | 1.36(4)* |
| F6 | 4f | 0.0845(3) | x | 0 | 1.36(4)* |
| F7 | 4f | 0.2586(3) | x | 0 | 1.36(4)* |

^a +, * constrained parameters.

Table 3. Selected interatomic distances (\AA) for Ba₂SrMg₄F₁₄ with estimated standard deviations in parentheses.

| | | | | | |
|--------|------|----------|--------|----------|----------|
| Mg1–F1 | (2×) | 1.948(4) | Mg1–F7 | 1.952(4) | |
| Mg1–F2 | (2×) | 2.012(3) | Mg1–F4 | 2.026(3) | |
| Mg2–F3 | | 1.868(5) | Mg2–F1 | (2×) | 1.981(3) |
| Mg2–F2 | (2×) | 1.993(3) | Mg2–F5 | | 2.033(5) |
| Sr2–F6 | (2×) | 2.367(3) | Sr2–F5 | (2×) | 2.568(3) |
| Sr2–F2 | (4×) | 2.587(3) | Ba1–F3 | | 2.480(5) |
| Ba1–F2 | (2×) | 2.772(3) | Ba1–F1 | (2×) | 2.785(3) |
| Ba1–F4 | | 2.932(4) | Ba1–F6 | | 2.934(4) |
| Ba1–F3 | | 2.951(5) | Ba1–F1 | (2×) | 3.041(3) |
| Ba1–F7 | | 3.043(4) | | | |

for corner-sharing octahedra in these and other compounds such as BaMgF₄ [3], BaSr(NH₄)Mg₅F₁₅ [7] and SrMgF₄ [8] vary from 3.5 to 4.2 \AA . The Mg–Mg distance increases as expected with increasing Mg–F–Mg angles from ~ 130 to 180° . In the title compound, the Mg–Mg distances have only a small variation of this value (3.618 to 3.693 \AA) related with the arrangement of symmetric building blocks, similar to the pyrochlore structure but with bridging fluorides isolating the Mg₄ units.

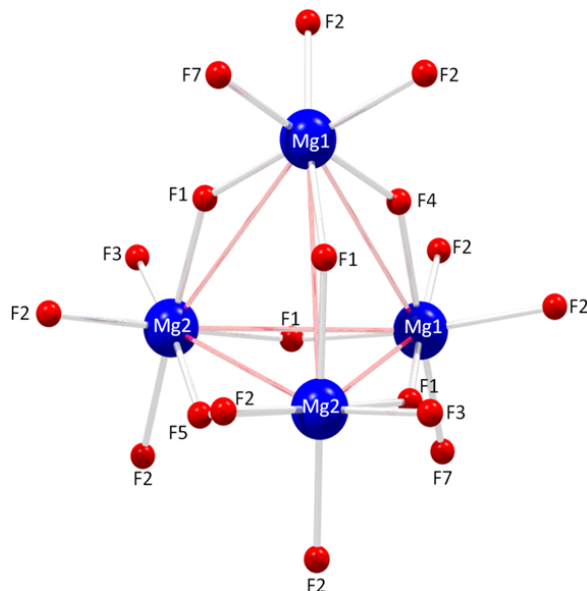


Fig. 2 (color online). View of the arrangement of a (MgF₆)₄ building block. The atoms F2 and F7 are connected to neighboring building blocks.

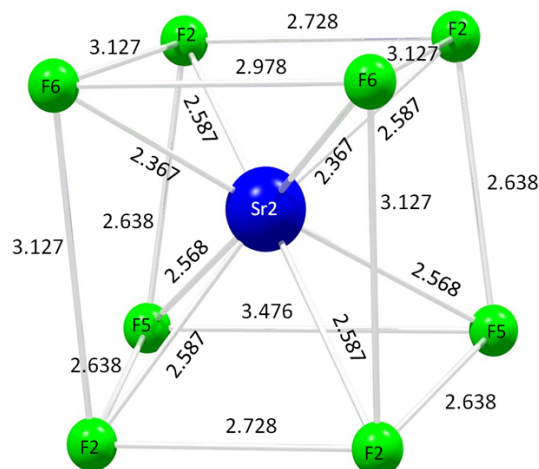


Fig. 3 (color online). View of the distorted cube around the Sr²⁺ ion in Ba₂SrMg₄F₁₄ with Sr–F and F–F distances in \AA .

In detail, the network is constructed from building blocks of four MgF₆ octahedra linked together into an empty tetrahedron (see Fig. 2). The same building block was found in the pyrochlore structure [9, 10], where the structure is formed by corner-sharing tetrahedra. In the title compound they are isolated and bridged by fluorine ions F2 and F7. The so-formed channels are occupied by 11-coordinate Ba²⁺ and 8-coordinate Sr²⁺ (see Fig. 3).

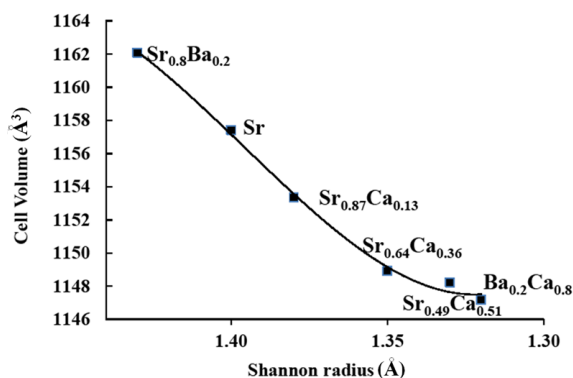


Fig. 4. Cell volumes of a series of compounds Ba₂MM'Mg₄F₁₄ as a function of averaged Shannon radii (compounds are designated by the elements MM' only).

The fluorine coordination in the network is tetrahedral with 2 Mg²⁺ and 2 Ba²⁺/Sr²⁺; only F3 has a triangular surrounding of 1 Mg²⁺ and 2 Ba²⁺. F6 is not connected to Mg²⁺ but is tetrahedrally surrounded by 2 Ba²⁺ and 2 Sr²⁺.

Pyrochlore and other related compounds with a channel structure are known to incorporate a variety of ions in their crystal structure. Here, the substitution can be understood on crystallochemical reasons based on (averaged) ion radii. The Shannon radii [11] for CN = 8 are Ba²⁺: 1.56, Sr²⁺: 1.40 and Ca²⁺: 1.26 Å. It was found that a solid solution of Ba²⁺ and Ca²⁺ in a ratio of ~ 1 : 5 (average radius of 1.32 Å) can be replaced with one Sr²⁺. The unit cell volumes follow this tendency as can be seen from Fig. 4. For the title compound, a higher value of 1157.4 Å³ was found as compared to 1147.2 Å³ for the Ca/Sr solid solution and 1162.1 Å³ for the Sr/Ba solid solution. Geometrical reasons as well as empirical energy calculations using the GULP package [12] allow predicting the formation of Sr/Ca solid solutions up to an amount to match the Ba/Ca structure [13]. Solid solutions could be prepared with a composition of Ba₂(Sr_{1-x}Ca_x)Mg₄F₁₄ with *x* = 0.13(1), nominal 0.25, 0.36(1), nominal 0.75 and 0.51(1), nominal 0.75. The highest Ca²⁺ concentration gives an average ionic radius of 1.33 Å and matches in its structural parameters with the solid solution stabilized in Ba₂(Ba_{0.2}Ca_{0.8})Mg₄F₁₄.

Experiments to replace Sr with Sr/Ba were carried out, and a solid solution limit of Ba₂(Sr_{0.83}(1)-Ba_{0.17}(1))Mg₄F₁₄ was observed. All data concerning volumes allow the determination of the stability range of solid solutions.

Table 4. Compositions of the analyzed samples as determined by powder diffraction analysis with e. s. d.'s in parentheses.

| Nominal stoichiometry | Observed phases | Abundances (wt.-%) |
|---|--|---|
| Ba ₂ SrMg ₄ F ₁₄ | Ba ₂ SrMg ₄ F ₁₄ (Ba,Sr)MgF ₄ | 99.6(1) 0.4(1) |
| Ba ₂ Sr _{0.75} Ca _{0.25} Mg ₄ F ₁₄ | Ba ₂ Sr _{0.87} Ca _{0.13} Mg ₄ F ₁₄ (Ba,Sr)MgF ₄ | 99.6(1) 0.4(1) |
| Ba ₂ Sr _{0.5} Ca _{0.5} Mg ₄ F ₁₄ | Ba ₂ Sr _{0.64} Ca _{0.36} Mg ₄ F ₁₄ (Ba,Sr)MgF ₄ | 99.6(1) 0.4(1) |
| Ba ₂ Sr _{0.25} Ca _{0.75} Mg ₄ F ₁₄ | Ba ₂ Sr _{0.49} Ca _{0.51} Mg ₄ F ₁₄ (Ca,Sr)F ₂ | 98.5(1) 1.5(1) |
| Ba ₂ Sr _{0.8} Ba _{0.2} Mg ₄ F ₁₄ | Ba ₂ Sr _{0.8} Ba _{0.2} Mg ₄ F ₁₄ (Ba,Sr)MgF ₄ | 89.9(3) 10.1(3) |
| Ba ₂ Sr _{0.6} Ba _{0.4} Mg ₄ F ₁₄ | Ba ₂ Sr _{0.8} Ba _{0.2} Mg ₄ F ₁₄ (Ba,Sr)MgF ₄ MgF ₂ Ba ₆ Mg ₇ F ₂₆ Ba ₆ Mg ₁₁ F ₃₄ Ba ₂ Mg ₃ F ₁₀ | 50.5(8) 16.3(7) 2.7(2) 5.0(4) 6.6(5) 18.9(5) |

The Sr²⁺ ion is localized in a distorted fluorine cube as can be seen from Fig. 3. The Sr–F and the F–F distances were compared for all solid solutions. Results are shown in Fig. 5. As expected, the dis-

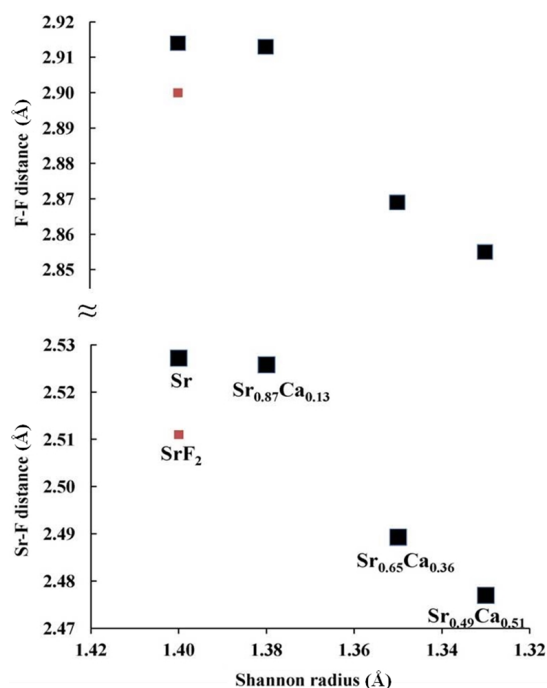


Fig. 5 (color online). Selected interatomic distances of a series of compounds Ba₂MM'Mg₄F₁₄ as a function of averaged Shannon radii (compounds are designated by the elements MM' only). Small squares are the values for SrF₂.

tances decrease with the amount of incorporated Ca²⁺. The same is true for the cell volume, which is illustrated in Fig. 4. Obviously, the curve flattens at higher Ca²⁺ concentrations, presumably because the structure reaches a geometrical limit and cannot be compressed further.

In all experiments the ratios of Sr²⁺ and Ca²⁺ ions aimed at could not be reached. Under the given synthesis conditions Ca²⁺ might partially remain in the solution as complexes. All chemical compositions of the phases are summarized in Table 4.

Doping with selected rare earth elements as Eu, Sm, Tb, Dy causes weak luminescent properties.

Conclusion

The structure of the novel compound Ba₂SrMg₄F₁₄ can be modified by local substitution within one chan-

nel with other alkaline earth ions. Substitution experiments followed by structural characterization of the powders show the stability range of this structure. The title compound Ba₂SrMg₄F₁₄ exhibits a volume variation of ~ 0.5 % by substitution showing the rigidity of the MgF₆ network. Different elements with similar average Shannon radii can be incorporated into this structure. The given solid solution potentials make this compound an interesting host material for luminescent rare earth elements.

Acknowledgements

The help of E. Eitenberger for SEM and EDX measurements, Dr. C. Gierl for DSC analysis, C. Knoll for IR measurements and E. G. Durak for her assistance in the synthesis is gratefully acknowledged.

-
- [1] F. Kubel, M. Pantazi, H. Hagemann, *Cryst. Res. Tech.* **2011**, *46*, 899–905.
- [2] TOPAS (version 4.2), Bruker AXS GmbH, Karlsruhe (Germany), **2009**.
- [3] F. Gingl, *Z. Anorg. Allg. Chem.* **1997**, *623*, 705–709.
- [4] F. Kubel, H. Hagemann, H. Bill, *Z. Anorg. Allg. Chem.* **1997**, *623*, 573–578.
- [5] W. Kerbe, M. Weil, F. Kubel, H. Hagemann, *Mater. Res. Bull.* **2004**, *39*, 343–355.
- [6] G. Vidal-Valat, J. P. Vidal, C. M. E. Zeyen, K. Kurki-Suonio, *Acta Crystallogr.* **1979**, *B35*, 1584–1590.
- [7] F. Kubel, M. Pantazi, *Z. Anorg. Allg. Chem.* **2007**, *633*, 752–756.
- [8] N. Ishizawa, K. Suda, B. E. Etschmann, T. Oya, N. Kodama, *Acta Crystallogr.* **2001**, *C57*, 784–786.
- [9] F. Kubel, B. Dundjerski, *Z. Anorg. Allg. Chem.* **2001**, *627*, 1589–1592.
- [10] E. A. Oliveira, I. Guedes, A. P. Ayala, J. Y. Gesland, J. Ellena, R. L. Moreira, M. Grimsditch, *J. Solid State Chem.* **2004**, *177*, 2943–2950.
- [11] R. D. Shannon, *Acta Crystallogr.* **1976**, *A32*, 751–767.
- [12] J. D. Gale, *J. Chem. Soc. Faraday Trans.* **1997**, *93*, 629.
- [13] F. Kubel, N. Wandl, M. Pantazi, results to be published.